Pressure boundary condition of the lattice Boltzmann method for fully developed periodic flows

Junfeng Zhang[1] and Daniel Y. Kwok[2,*]
[1]*Department of Biomedical Engineering, School of Medicine, Johns Hopkins University, Baltimore, Maryland 21205, USA*
[2]*Nanoscale Technology and Engineering Laboratory, Department of Mechanical Engineering, Schulich School of Engineering, University of Calgary, Calgary, Alberta, T2N 1N4, Canada*
(Received 27 October 2005; published 11 April 2006)

The general periodic boundary condition for the lattice Boltzmann method has been modified to incorporate the pressure difference for fully developed periodic flows. The results demonstrated that, unlike other existing pressure boundary treatments, the proposed procedure/treatment does not generate nonphysical inlet and outlet flow disturbances while preserving the system periodicity. This method is readily applicable to a range of lattice Boltzmann simulations for systems with periodic electric potential and temperature fields.

DOI: 10.1103/PhysRevE.73.047702 PACS number(s): 02.70.−c, 47.11.−j, 47.60.+i, 47.85.Np

The lattice Boltzmann method (LBM) has experienced rapid development in recent years [1–4] to simulate various hydrodynamic systems. Along with the LBM development, tremendous efforts have been devoted to develop accurate and efficient boundary schemes for different situations [5–18]. As for other simulation techniques, however, boundary conditions (BCs) play a crucial role for meaningful LBM simulations. Due to the particle-based nature of LBM, BCs are implemented by specifying the unknown particle distribution functions entering the simulation domain, instead of the macroscopic fluid properties, such as velocity and pressure. This imposes a restriction on the LBM to simulate meaningful hydrodynamic systems, where the pressure gradient is commonly utilized to induce fluid motions.

Dupuis [18] examined the different LBM methods of applying a pressure difference to a simple Poiseuille flow, and found that they usually produced unphysical and largely false inlet/outlet velocity/pressure disturbance. Such a phenomenon was also reported elsewhere [19,20]. Among these studies, the only method not suffering from this defect is the one that replaces the pressure gradient by an equivalent body force which is, however, only valid for channels with a uniform cross-sectional area. On the other hand, Zou and He [10] derived the pressure and velocity BCs by assuming a bounce-back mechanism for nonequilibrium distributions on the boundary nodes. For the inlet/outlet boundary, they assumed the transverse velocities to be zero, which is, in general, not valid for most situations. Other schemes have also been proposed to impose a pressure difference across the inlet and outlet of the simulation domain [6,9]. However, system periodicity was not properly incorporated.

Figure 1 illustrates the schematic of a duct flow with periodic rectangular disturbances. Many experimental studies have revealed that the entrance lengths of fluid flow in such streamwise-periodic systems are short and the flow can often become fully developed in three to five periods [21]. Hence, the flow velocity $\mathbf{u}$ and pressure P in such systems exhibit periodic behaviors as follows [22]:

$$\mathbf{u}(x,y) = \mathbf{u}(x+nL,y), \quad P(x,y) = P(x+nL,y) + n\beta L, \quad (1)$$

where n can be any integer, L is the period along the x direction for periodicity, and β is a constant representing the overall pressure gradient along the periodic direction. A similar relation for temperature also exists [22]. In this paper, a LBM pressure boundary treatment for fully developed periodic flows is developed which is applicable to a wide range of systems with geometric periodicity, such as corrugated ducts [22,23], compact heat exchangers [24], filtration [25], fuel cells [26], and microchannels [27,28]. In order to demonstrate the validity of the BCs, simulations will also be presented for flows in uniform and nonuniform channels.

For the purpose of completeness, a brief description of LBM is given in this section. Generally, after discretization in time and space, the lattice Boltzmann equation with a Bhatnagar–Gross–Krook collision term can be written as [3]

$$f_i(\mathbf{x}+\mathbf{e}_i, t+1) - f_i(\mathbf{x},t) = -(1/\tau)[f_i(\mathbf{x},t) - f_i^{\mathrm{eq}}(\mathbf{x},t)], \quad (2)$$

where the distribution function $f_i(\mathbf{x},t)$ denotes fluid particle population moving in the lattice direction $\mathbf{e}_i$ at a lattice site $\mathbf{x}$ and a time step t; τ is the collision time, and $f_i^{\mathrm{eq}}(\mathbf{x},t)$ is a prescribed equilibrium distribution function of fluid density ρ and velocity $\mathbf{u}$, which are defined, respectively, as follows

$$\rho = \sum_i f_i, \quad \rho\mathbf{u} = \sum_i f_i \mathbf{e}_i. \quad (3)$$

There are several lattice structures available [18]. In this work, we have employed a square two-dimensional nine-

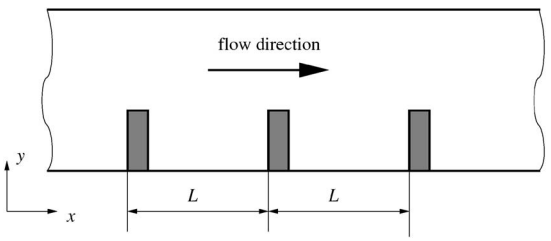

FIG. 1. A schematic of a duct with periodic rectangular disturbances.

*Author to whom correspondence should be addressed. Electronic address: daniel.kwok@ucalgary.ca

 ©2006 The American Physical Society

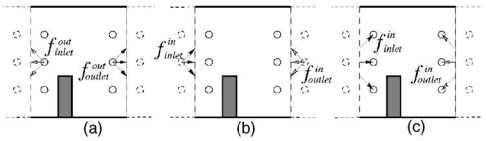

FIG. 2. Modification of the general periodic BC to account for pressure difference between two adjacent domains.

velocity (D2Q9) model for its simplicity. The nine discrete lattice velocities are given by

$$\mathbf{e}_0 = \mathbf{0},$$

$$\mathbf{e}_i = (\cos[(i-1)/2]\pi, \sin[(i-1)/2]\pi), \quad i = 1-4, \tag{4}$$

$$\mathbf{e}_i = \sqrt{2}(\cos[(2i-9)/4]\pi, \sin[(2i-9)/4]\pi), \quad i = 5-8;$$

and the equilibrium distribution functions can be expressed as

$$f_i^{\mathrm{eq}} = \rho\alpha_i\left[1 + 3\mathbf{e}_i \cdot \mathbf{u} + \tfrac{9}{2}(\mathbf{e}_i \cdot \mathbf{u})^2 - \tfrac{3}{2}u^2\right], \tag{5}$$

with $\alpha_0 = 4/9$, $\alpha_{1-4} = 1/9$, and $\alpha_{5-8} = 1/36$. Macroscopic continuity and momentum (Navier–Stokes) equations can be obtained from the microdynamics defined above through the Chapman–Enskog procedure [2,3]. The fluid pressure P and viscosity ν in the resulting Navier–Stokes equation are defined, respectively, as

$$P = c_s^2\rho, \quad \nu = c_s^2(2\tau - 1)/2, \tag{6}$$

where the sound speed c_s is given by $c_s^2 = 1/3$ for a D2Q9 lattice model.

The general periodic BCs are commonly employed in particle-based simulations, such as molecular dynamics, Monte Carlo simulations, LBM, and dissipative particle dynamics. Under such treatment, a particle leaving the domain across a boundary will enter from the opposite side. Therefore, the simulated system will consist of identical domains. However, in the fully developed periodic flows described above, there is an overall pressure difference between the domain and its adjacent image domain; and hence modifications of the original periodic BCs are necessary to account for such a difference.

The description of flow periodicity from Eq. (1) can be rewritten as the following BCs for an appropriately selected simulation domain, which includes only one period of the physical system:

$$\mathbf{u}(x=0,y) = \mathbf{u}(x=L,y), \quad P(x=0,y) = P(x=L,y) + \beta L. \tag{7}$$

Due to the relationships between the distribution f's and fluid properties $\mathbf{u}$ and ρ [Eq. (3)] at a lattice node, multiplying the distribution f's by a factor γ will change the density ρ to $\gamma\rho$, while the velocity remains unaffected. On the other hand, the fluid pressure in the resulting Navier–Stokes equation [see Eq. (6)] is proportional to the density (i.e., $P = c_s^2\rho$); and thus the pressure gradient can be implemented as a corresponding density gradient [10,18].

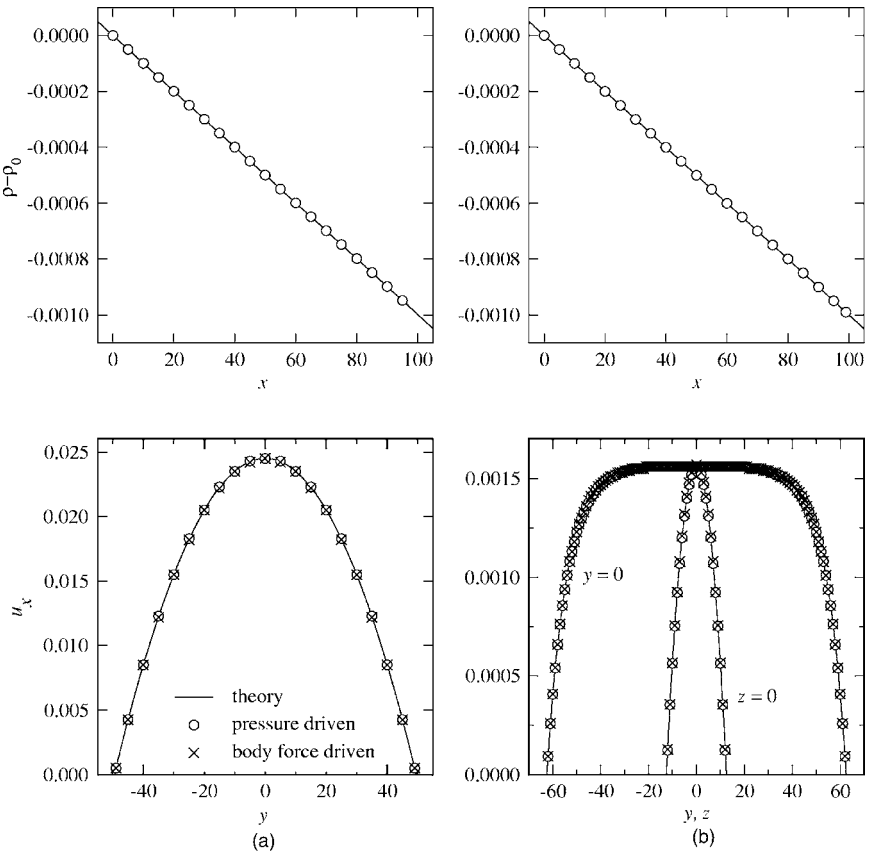

FIG. 3. Density distributions (upper panels) and axial velocity u_x profiles (lower panels) of 2D (a) and 3D (b) channel flows. The symbols are LBM results (○ for the pressure driven flow and × for the body force driven flow), and the solid lines are from fluid mechanics theory [29,30].

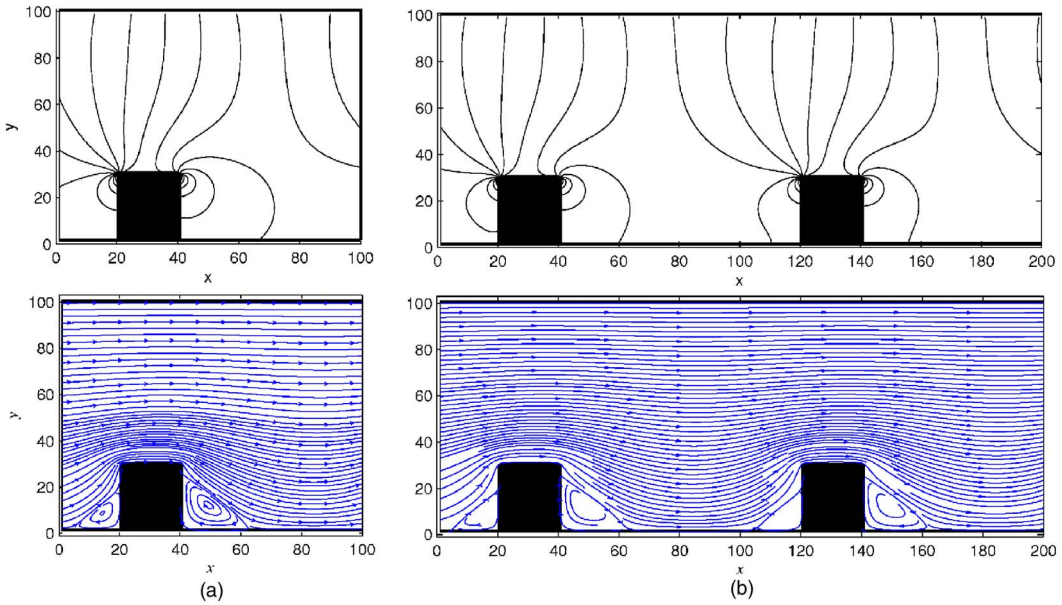

FIG. 4. (Color online) Density contours (upper panels) and flow fields (lower panels) obtained over L (a) and $2L$ (b) domains.

Let us consider the distributions leaving the outlet boundary after collision $f_{\text{outlet}}^{\text{out}}$ [normal filled arrows in Fig. 2(a)]. Their images $f_{\text{inlet}}^{\text{in}}$ in the upstream imaginary domain [sharp filled arrows in Fig. 2(b)] should produce the same velocity and density difference of $\beta L/c_s^2$. These imaginary distributions $f_{\text{inlet}}^{\text{in}}$ will then propagate across the inlet boundary of the simulation domain and arrive at the inlet nodes [sharp filled arrows in Fig. 2(c)]. Similar procedures can also be applied to the distributions leaving the inlet boundary ($f_{\text{inlet}}^{\text{out}}$ and $f_{\text{outlet}}^{\text{in}}$, open arrows in Fig. 2). In addition, a reference pressure/density is necessary, and this is represented by setting the average density of the column on the right of the inlet nodes as $\rho_0+\beta/c_s^2$. Based on this description, the LBM BC can be expressed mathematically as follows:

$$f_{\text{inlet}}^{\text{in}} = f_{\text{outlet}}^{\text{out}} \frac{\rho_0 + \beta/c_s^2}{\bar{\rho}_{\text{outlet}}}, \quad f_{\text{outlet}}^{\text{in}} = f_{\text{inlet}}^{\text{out}} \frac{\rho_0 - \beta L/c_s^2}{\bar{\rho}_{\text{inlet}}}, \qquad (8)$$

where $\bar{\rho}_{\text{inlet}}$ and $\bar{\rho}_{\text{outlet}}$ are the density averages over the inlet and outlet column, respectively.

To validate the proposed BC, pressure driven Poiseuille flows in two-dimensional (2D) (width $W=99$) and three-dimensional (3D) (width $W=25$ and height $H=125$) uniform channels are simulated. We employed the D2Q9 lattice model for 2D and D3Q19 (three-dimensional nineteen-velocity) [1] for 3D simulations. The typical half-way bounce-back BC for the solid surfaces was employed [1] with an initial density distribution of $\rho=1$, $\tau=1$, and $\beta/c_s^2=10^{-5}$. The density distributions along the channel axis (○, upper panels) and velocity profiles across the channel (○, lower panels) are displayed in Fig. 3. Linear fittings of the density distributions (solid lines, upper panels in Fig. 3) produce a density gradient of 1×10^{-5}, which is in agreement with the simulation setup $\beta/c_s^2=10^{-5}$. Unlike those presented in [18], the density (pressure) gradient from this proposed BC is uniform along the channel, and no inlet/outlet effects are observed (upper panels in Fig. 3). For comparison, LBM results from the equivalent body force driven flows (×) and analytical predictions [29,30] (solid lines) are also shown in the lower panels in Fig. 3. The corresponding Reynolds numbers $\text{Re}=u_{x,\max}W/\nu$ are 14.6 for the 2D flow and 0.234 for the 3D flow. In such uniform channels, the LBM results for the pressure driven and the body force driven flows are identical and they both agree well with the theoretical predictions.

In addition, to demonstrate that this modified periodic BC represents system periodicity correctly, we simulated the system shown in Fig. 1 by selecting the domains to include the length of the duct as L and $2L$. Figure 4 displays the density contours (upper panels) and corresponding velocity fields (lower panels). No difference in the patterns obtained from these two different domains can be found. For example, typical flow features are all captured, including the higher-pressure regions upstream the disturbances, lower-pressure regions downstream the disturbances, and vortexes near the bottom of the disturbances. For regions above the rectangular disturbances ($y>60$), density decreases linearly along the channel while all streamlines are roughly parallel, suggesting that the effects of disturbances on the flow properties are smaller.

A more quantitative comparison can be performed on the density (pressure) and velocity profiles along the duct at three transverse positions, $y=20$ (black rectangle), 50 (blue triangle), and 70 (red circle), and is plotted in Fig. 5. It can be seen that the results from two different domains (symbols for the $1L$ domain and solid lines for the $2L$ domain in Fig. 5) are nearly identical. Here, the Reynolds number $\text{Re}=u_{x,\max}W/\nu=9.09$. A LBM simulation of the equivalent body force driven flow in the $2L$ domain has also been conducted, and the velocities are shown as dashed lines in Figs. 5(b) and 5(c). The body force here $g=3.54\times10^{-6}$ is obtained by equalizing the total body force to the external force due to the pressure difference across the domain inlet/outlet [31]. It

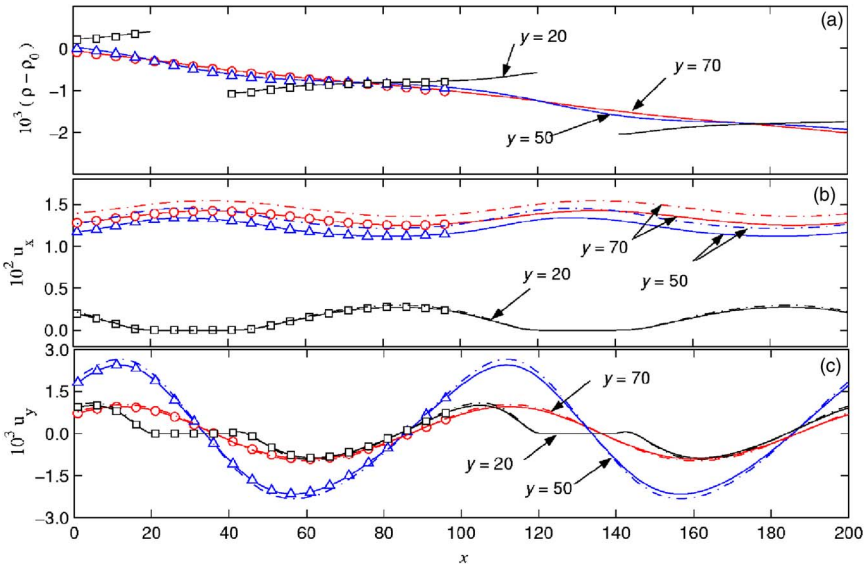

FIG. 5. (Color online) Profiles of density difference $\rho-\rho_0$ (a) and velocity u_x (b) and u_y (c) along a duct at three different transverse positions ($y=20$ in black rectangle, 50 in blue triangle, and 70 in red circle) with domains consisting L (symbols) and $2L$ (solid lines). The velocities of the equivalent body force driven flow in the $2L$ domain are also displayed (dashed lines) in (b) and (c). Note that there is no fluid density, and the velocities are zero in the space occupied by the disturbances ($19<x<40$ and $119<x<140$; $0<y<30$).

should be noted that, according to such an approach, the equivalent body force depends on the domain position. For example, if we select the inlet at $x=30$ (see Fig. 4), then $g=2.50\times10^{-6}$. Such different body forces will definitely produce different flow fields, and this is not physically realistic. Here, the velocities from body force $g=3.54\times10^{-6}$ are in general larger than those from the original pressure gradient. It was also found that, under the case of periodic disturbances, the transverse velocity is nonzero at both the inlet and outlet [Fig. 5(c)]. Thus, existing treatments, either by replacing the pressure gradient with a body force or by Zou's nonequilibrium bounce-back mechanism [10], are not applicable to such pressure-driven flows in general periodic systems.

In summary, a modified periodic BC for LBM has been developed for fully developed periodic flows. Simulations show that system periodicity was well represented and no inlet/outlet effect was observed. We have also compared our pressure boundary treatment with the equivalent body force driven flows and found that these two approaches agree with each other only for uniform channels. Therefore, replacing a pressure gradient with an equivalent body force is not appropriate for the general periodic systems. The proposed boundary treatment is also better than other existing techniques in term of inlet/outlet effects. By removing the inlet/outlet effects on velocity/density, our boundary treatment will also improve the simulation stability. The described procedures for periodic pressure boundaries can be readily extended to temperature and electric fields situations.

This work was supported by the Natural Sciences and Engineering Research Council of Canada (NSERC).

[1] S. Succi, *The Lattice Boltzmann Equation* (Oxford University Press, Oxford, UK, 2001).
[2] Y. H. Qian *et al.*, in *Ann. Rev. Compt. Phys. III*, edited by D. Stauffer (World Scientific, Singapore, 1995), pp. 195–242.
[3] S. Chen and G. D. Doolen, Annu. Rev. Fluid Mech. **30**, 329 (1998).
[4] J. Zhang and D. Y. Kwok, J. Comput. Phys. **206**, 150 (2005).
[5] P. A. Skordos, Phys. Rev. E **48**, 4823 (1993).
[6] T. Inamuro *et al.*, Phys. Fluids **7**, 2928 (1995).
[7] D. Noble, *et al.*, Phys. Fluids **7**, 203 (1995).
[8] S. Chen *et al.*, Phys. Fluids **8**, 2527 (1996).
[9] R. Maier *et al.*, Phys. Fluids **8**, 1788 (1996).
[10] Q. Zou and X. He, Phys. Fluids **9**, 1591 (1997).
[11] R. Mei *et al.*, J. Comput. Phys. **155**, 307 (1999).
[12] R. Verberg and A. J. C. Ladd, Phys. Rev. Lett. **84**, 2148 (2000).
[13] A. Wagner and I. Pagonabarraga, J. Stat. Phys. **107**, 521 (2002).
[14] S. Ansumali and I. V. Karlin, Phys. Rev. E **66**, 026311 (2002).
[15] Z. Guo *et al.*, Phys. Fluids **14**, 2007 (2002).
[16] S. Succi, Phys. Rev. Lett. **89**, 064502 (2002).
[17] J. Zhang and D. Y. Kwok, Phys. Rev. E **70**, 056701 (2004).
[18] A. Dupuis, Ph.D. thesis, Université de Genève (2002).
[19] S. Marconi *et al.*, Int. J. Mod. Phys. C **14**, 1015 (2003).
[20] Z. Guo *et al.*, J. Chem. Phys. **122**, 144907 (2005).
[21] Z. X. Yuan *et al.*, Int. J. Numer. Methods Fluids **28**, 1371 (1998).
[22] S. V. Patankar *et al.*, ASME J. Heat Transfer **99**, 180 (1977).
[23] R. S. Amano, ASME J. Heat Transfer **107**, 564 (1985).
[24] C. Nonino and G. Comini, Numer. Heat Transfer, Part B **34**, 361 (1998).
[25] S. Chen *et al.*, Comput. Mech. **28**, 152 (2002).
[26] T. A. Trabold, Heat Transfer Eng. **26**, 3 (2005).
[27] G. Croce and P. D'Agaro, Superlattices Microstruct. **35**, 601 (2004).
[28] F. Lu *et al.*, J. Phys. Chem. B **108**, 14970 (2004).
[29] F. M. Write, *Fluid Mechanics* (McGraw-Hill, New York, 1979).
[30] P. Gondret *et al.*, Phys. Fluids **9**, 1841 (1997).
[31] D. Kandhai, *et al.*, J. Comput. Phys. **150**, 482 (1999).